

RESEARCH

Open Access



Identification of mRNA biomarkers in extremely early hypertensive intracerebral hemorrhage (HICH)

Haidong Gao^{1†}, Jian Zhang^{1†}, Xinjun Wang^{1*}, Jixin Shou^{1*}, Jianye Wang¹ and Peng Yang¹

Abstract

Introduction Hypertensive intracerebral hemorrhage (HICH) stands out as a critical complication of primary hypertension. Consequently, investigating messenger RNA (mRNA) biomarkers becomes imperative, offering potential targets. This study is conducted for elucidating the expression profile of blood mRNA biomarkers in HICH.

Methods Twenty-five HICH patients were constituted the HICH group. Twenty-two healthy volunteers recruited and comprised the control group. Peripheral blood cells were extracted to identify candidate mRNA. The identified differential expressions of genes between the two groups were validated, and the potential associations between these differentially expressed genes and adverse events were analyzed. GO and KEGG enrichment of DEGs, Weighted Gene Co-expression Network and Protein Interaction Network were established. target mRNA was screened.

Results The study identified 3163 differentially expressed genes in HICH. 8 candidate mRNA (SPI1, HK3, HCK, SYK, CD14, FCER1G, CYBB, FGR) were pinpointed. Associations with pathways affecting HICH development included HIF-1 signaling, NF-kappa B signaling, and C-type lectin receptor signaling. In the HICH group, higher expressions of HK3, HCK, SYK, CD14, FCER1G, CYBB, and FGR, and lower SPI1 expression compared to the control group. HICH patients experienced high rates of complications: pulmonary infection (84%), epilepsy (16%), enlarged hematoma (20%), gastrointestinal bleeding (48%), malnutrition (84%), and lower limb deep vein thrombosis (DVT) (12%). Factors contributing to pulmonary infection included age and elevated expression of HCK, SYK, CD14, and FGR. SPI1 was associated with epilepsy, while its lower expression correlated with hematoma enlargement. Gastrointestinal bleeding was linked to increased cerebral hemorrhage. Malnutrition was associated with higher age, and expressions of HK3, HCK, SYK, CD14, FCER1G, CYBB, and FGR. Patients with lower limb DVT had elevated expressions of the identified genes.

Conclusion In hypertensive intracerebral hemorrhage, there are elevated expressions of HK3, HCK, SYK, CD14, FCER1G, CYBB, and FGR, along with reduced expression of SPI1. Furthermore, age, along with elevated expressions of HCK, SYK, CD14, and FGR, serves as influencing factors contributing to pulmonary infection in patients.

Keywords High throughput sequencing of next-generation RNA, Hypertensive cerebral hemorrhage, Messenger ribonucleic acid, Weighted gene co-expression network analysis

[†]Haidong Gao and Jian Zhang co-first author.

*Correspondence:

Xinjun Wang
wangxinjun2045001@163.com

Jixin Shou
Shoujx2024001@163.com

Full list of author information is available at the end of the article



Introduction

Seventy-five percent of patients with acute cerebral hemorrhage have hypertension [1]. Hypertensive intracerebral hemorrhage (HICH) is one of the most critical complications of primary hypertension, with a high mortality and disability rate [2]. Patients with cerebral hemorrhage usually have extremely poor prognosis and limited treatment options. The direct occupation and compression of hematoma after bleeding are the causes of mechanical damage to brain tissue, and excessive activation of inflammation, cell apoptosis, autophagy, and other factors in the brain tissue surrounding the hematoma are important reasons for secondary damage to brain tissue [3]. The neurological dysfunction of patients with cerebral hemorrhage is mainly caused by the degeneration, necrosis, or apoptosis of nerve cells around the hematoma, and these pathological processes are closely related to gene expression and regulation [4]. Research has shown that biomarkers can predict the development and prognosis of cerebrovascular diseases and play a crucial mediating role in the prognosis of neuronal damage, brain edema, and neurological function [5]. However, its specific mechanism is still not very clear. Therefore, it is necessary to further clarify the molecular mechanisms underlying the occurrence and development of cerebral hemorrhage, and search for potential molecular therapeutic targets and diagnostic markers for early screening.

Recently, researchers have used gene chip technology to analyze genes in patients with cerebral hemorrhage and hypertension and obtained 340 differential genes (DEGs) [6]. There have been studies on the gene expression profile of cerebral hemorrhage. Through microarray analysis, 399 DEGs were obtained between the surrounding tissue of the hematoma and the contralateral gray matter, and 756 DEGs were identified between the surrounding tissue of the hematoma and the contralateral white matter. There are a total of 35 common DEGs in both groups [7]. By using weighted gene co-expression network analysis, potential gene co-expression modules were explored for the progression of spontaneously hypertensive intracerebral hemorrhage in mice, with 554 genes exhibiting abnormal expression [8]. However, there have been no relevant reports on the altered expression of messenger ribonucleic acid (mRNA) and its possible clinical significance in extremely early hypertensive intracerebral hemorrhage in the basal ganglia region.

In this study, we enrolled peripheral blood samples from patients with hypertensive intracerebral hemorrhage in the basal ganglia region and a healthy control population and conducted RNAseq analysis. Then, comprehensive bioinformatics methods including weighted gene co-expression network analysis (WGCNA) and protein interaction database analysis (PPI) were used

to identify candidate mRNA [9]. Finally, the possible mechanisms of candidate mRNA expression in the HICH process were elucidated through Gene Ontology (GO) terminology, Kyoto Encyclopedia of Genes and Genomes (KEGG) pathway enrichment analysis, and Gene Set Enrichment Analysis (GSEA) [10–13], and the differential expressions of genes in patients with hypertensive intracerebral hemorrhage in the basal ganglia region and healthy controls were verified, then the possible relationship between differentially expressed genes and adverse events were analyzed in patients.

Patient selection

Twenty-five emergency surgical patients (9 females and 16 males) diagnosed with HICH in the basal ganglia region were carefully chosen from the Neurosurgery Department of the Fifth Affiliated Hospital of Zhengzhou University. The HICH group, with an average age of (69.92 ± 4.56) years old, comprised individuals eligible for admission if diagnosed with primary basal hemorrhage (putamen or thalamus) within 6 h of onset, meeting surgical indications regarding the extent of bleeding. Neurosurgeons diagnosed HICH based on acute symptoms and CT brain scans. Approval for this method was granted by the Ethics Committee of the Fifth Affiliated Hospital of Zhengzhou University (Approval No. Y2021052), or written informed consent was obtained from the patient's representative. Additionally, 22 healthy volunteers (9 females and 13 males) of comparable age (average age of (68.86 ± 4.35) years old) were recruited as the control group during the same period. Exclusion criteria involved patients with intracerebral hemorrhage secondary to brain trauma, tumors, vascular malformations, or anticoagulant use.

Materials and methods

Blood sample collection and cell sample extraction

Patients in the HICH group received peripheral blood samples before starting treatment after admission, while healthy controls received peripheral blood samples the day after inclusion in the study. Blood samples were taken using blood routine EDTA-K2 anticoagulant tubes. Extract blood cell samples from blood samples within 12 h. Step: (1) Add an equal volume of PBS (1x) to fresh whole blood and mix thoroughly. (2) Slowly transfer to another centrifuge tube that has already added peripheral blood lymphocyte separation solution and keep the above mixture above the lymphocyte separation liquid level, then place it in TDL_Centrifuge at 2200 g for 30 min at 18 °C in a 5 M centrifuge. (3) Carefully separate the white blood cell layer using a pipette, wash the white blood cells with PBS (1x), centrifuge to recover the white blood cells, and discard the

supernatant. (4) Add 20 times the volume of pre-cooled TRIzol reagent to the white blood cells, repeatedly blow the cells until the clumps of cells are not visible, and the entire solution is in a clear and non-viscous state. Quickly fix the extracted cell sample in liquid nitrogen for 20 min and transfer it to a -80°C refrigerator for storage.

RNA extraction, library construction, and sequencing

Following the manufacturer's guidelines, total RNA was extracted using TRIzol reagent kit (Invitrogen). The RNA's quality was assessed with the Agilent 2100 biological analyzer (Agilent Technologies, CA, USA), employing agarose gel electrophoresis without ribonuclease for detection. After extracting total RNA, oligomeric (DT) beads were used to enrich eukaryotic mRNAs, and RiboZero™ magnetic reagent kit (Epi-Center, WI, USA) was used to remove rRNA to enrich prokaryotic mRNAs. Subsequently, the concentrated mRNA fragments underwent conversion into short sequences using fragment buffer and were reverse transcribed into cDNAs via random primers. Second-stranded genes were synthesized using DNA polymerase I, ribonuclease H, dNTP, and buffer. Purification of DNA fragments ensued using the QiaQuick polymerase chain reaction kit (Qiagen, Venlo, Holland), with subsequent repair of base ends and connection of Illumina sequencing connectors. The size of the junction product was determined through agarose gel electrophoresis, followed by amplification of the product using polymerase chain reaction (PCR) to establish a cDNA library.

The library was sequenced by Gene Denovo Biotechnology Co., Ltd. on the Illumina Sequencing Platform (Illumina HiSeq™ 2500) using paired terminal technology [14]. FastP program was written to select clean reads by removing low-quality sequences (more than 50% of bases with a mass lower than 20% in a sequence), read with more than 10% N bases (bases unknown), and read containing splice sequences. HISAT2 was used for the alignment of sequence readings and assembly of the Bactrian camel genome (GOV/GENAME/Term = Camelus + Bactrianus) as a reference genome. Then, based on gene expression information, principal component analysis was performed using R to calculate the Pearson correlation coefficient. Then, differential gene expression analysis was performed using DESeq2 software, and related pathways were studied using KEGG and GO analysis. In addition, the string protein interaction database was used to analyze the interactions and relationships between proteins of interest. Established a differential gene protein interaction network.

Differential expression genes (DEG)

The differential expression between the two groups was analyzed using DESeq2 software (and analyze the differential expression between the two groups of samples using Edger software) [13]. Genes/transcripts with EDR parameters less than 0.05 and absolute folding change ≥ 2 are considered differentially expressed. Thus, statistically significant differential genes were identified between the hypertensive intracerebral hemorrhage group and the primary hypertension group.

GO and KEGG enrichment analysis of DEGs

GO functional analysis was used for GO functional classification annotation and enrichment analysis of differentially expressed genes. Map differentially expressed genes to each term in the GO database (<http://www.geneontology.org/>) and calculate the number of genes for each term to obtain a list of genes with a certain GO function and the number of genes. Then, a hypergeometric test is applied to search for GO entries that are significantly enriched in differentially expressed genes compared to the entire background gene. The p -value calculation formula for this hypothesis test is:

$$P = 1 - \sum_{i=0}^{m-1} \frac{\binom{M}{i} \binom{N-M}{n-i}}{\binom{N}{n}}$$

Among them, N is the number of genes with GO annotation among all background genes. n is the number of differentially expressed genes in N . M is the number of genes annotated as a specific GO term among all background genes. m is the number of differentially expressed genes annotated as a specific GO term. After Bonferroni correction, the calculated p -value is defined as GO terms that are significantly enriched in differentially expressed genes, with a corrected p -value ≤ 0.05 as the threshold. The main biological functions exercised by differentially expressed genes can be determined through GO functional significance enrichment analysis.

KEGG enrichment analysis of core module genes using the 'clusterProfiler' package of R software. Pathway significance enrichment analysis used the KEGG pathway as a unit and used hypergeometric tests to identify pathways where differentially expressed genes were significantly enriched compared to background genes. The calculation formula was the same as the GO analysis. Here N is the number of genes with Pathway annotations among all background genes. n is the number of differentially expressed genes in N . M is the number of genes annotated as a specific pathway among all background genes. m is the differential expression of the number of specific Pathway annotation genes. After multiple tests and correction, Pathways with Q -value ≤ 0.05 were defined as

significantly enriched Pathways in differentially expressed genes. The Q-value here is the *p*-value after error detection rate (EDR) correction.

Analysis of weighted gene co-expression network

R language pack was used for WGCNA algorithm analysis [15]. A one-step method was used to construct a weighted gene co-expression network for DEGs. The optimal soft threshold was obtained by calculating the Pearson correlation coefficient between genes, i.e. β . The network closer was made to scale-free networks. Then, the adjacency matrix was transformed into a topological overlap matrix (TOM), and the dissimilarity between genes was calculated as $\text{disTOM} = 1 - \text{TOM}$ to achieve hierarchical clustering. Finally, dynamic cutting was used to merge similar modules.

Construction of protein interaction network and screening of target mRNA

We crossed and intersected the central genes in the key modules with the differentially expressed genes in the hypertensive intracerebral hemorrhage group as the target gene set. We applied the interaction relationships in the STRING protein interaction database to analyze the differentially expressed gene protein interaction network. We will import the selected target gene set into the STRING website and export the PPI network data to a TSV file. Then we used Cytoscape software to analyze and visualize the interaction network, identifying the key genes that play an important role in the PPI network, and these key genes are the target mRNA we want to screen [16].

Functional analysis of target mRNA

We conducted GO terminology and KEGG pathway enrichment analysis on the central genes in the key modules to identify the pathways in which the central genes are mainly enriched. Then, we conducted pathway enrichment analysis on the target mRNA again to determine the main pathway in which the target gene is located and further explored the function of the target gene.

Verification of SPI1, HK3, HCK, SYK, CD14, FCER1G, CYBB, FGR gene expressions

5 ml of peripheral blood from two groups were taken, centrifuge at 4000r/min for 8 min, and real-time fluorescence quantitative polymerase chain reaction was used to measure the expressions of SPI1, HK3, HCK, SYK, CD14, FCER1G, CYBB, and FGR in the supernatant. The internal reference was GAPDH, and the

Table 1 Gene primer information

Genes	Primer sequence	Amplification product length (bp)
SPI1	Forward: 5'-AGCAGATGCACGTCCTCG ATAC-3' Reverse: 5'-TCTTCTTCTTGCTGCTGTCTC-3'	237
HK3	Forward: 5'-TGGGTGACTCTAACTGGCATTG-3' Reverse: 5'-AATGAGGGTGCTCTGTCCA-3'	228
HCK	Forward: 5'-CCGAAGCACCTTCAGCACTCT-3' Reverse: 5'-ATCTCCCAGGCATCTTTCTCC-3'	135
SYK	Forward: 5'-GAGCAGGCCATCATCAGTCAG-3' Reverse: 5'-CGGATCAGGAACCTTTCCA TTTGT-3'	155
CD14	Forward: 5'-AGCCTAGACCTCAGCCAC AACT-3' Reverse: 5'-CCCAGCGAACGACAGATTG-3'	105
FCER1G	Forward: 5'-GCAGTGGTCTTGCTTTACTC CTTT-3' Reverse: 5'-GACAGTAGAGGAGGGTGA GGACA-3'	124
CYBB	Forward: 5'-ATGAGGTGGTATGTTAG TGGGA-3' Reverse: 5'-TTTGAGCTTCAGATTGGTGGC-3'	110
FGR	Forward: 5'-GACCCTGTTTCATTGCCCTGTA-3' Reverse: 5'-TCTCCAATCTTTCCAAAGTACC- 3'	217
GAPDH	Forward: 5'-GGAAGCTTGTCATCAATGGAA ATC-3' Reverse: 5'-TGATGACCCTTTGGCTCCC-3'	168

primers used are shown in Table 1. ConFig. the reaction system, perform PCR, and draw dissolution and amplification curves. Calculate $2^{-\Delta\Delta C_t}$.

Diagnosis of adverse events in the HICH group

HICH patients receive routine treatment, including minimally invasive hematoma removal surgery, hypotension, reducing brain edema, nutritional support, and infection prevention. Adverse events include lung infection, epilepsy, hematoma enlargement, gastrointestinal bleeding, malnutrition, and lower limb DVT.

Statistical analysis

SPSS software (version 26.0) was used for statistical analysis of the data. The measurement data were verified to follow a normal distribution using the K-S method, described as ' $\bar{x} \pm s$ ', and compared between groups using independent sample t-tests. The counting data were described as "rate/%" and inter-group comparisons were conducted using χ^2 tests. Logistic regression analysis was used to explore the risk factors for various adverse events in patients. $P < 0.05$ indicated a statistically significant difference.

Results

Comparison of baseline features between two groups

There was no statistically significant difference in gender, age, and smoking history between the two groups ($P > 0.05$). The systolic and diastolic blood pressure in the HICH group were higher than those in the control group ($P < 0.05$), as shown in Table 2.

DEGs in peripheral blood of patients with hypertensive intracerebral hemorrhage and primary hypertension

We detected a total of 19,014 genes in all samples and conducted RNA differential expression analysis between two different groups using DESeq2 software (as well as between two samples using edgeR). Genes with an EDR parameter below 0.05 and an absolute multiple change of ≥ 2 are considered differentially expressed. Among the 19014 mRNA detected by us, there were 3163 DEGs between the HICH group and the hypertension group, including 1777 upregulated DEGs and 1386 downregulated DEGs. The distribution of DEG was visualized as a volcanic map and a hierarchical clustering heat map (Fig. 1).

GO and KEGG analysis of DEGs

We conducted GO and KEGG analysis on all differentially expressed genes. According to GO analysis, DEGs were mainly involved in the activation of inflammatory cells and the regulation of immune responses in the BP term. These genes were mainly enriched in the vesicle transport, cytoplasmic portion, and endometrial system in the CC term, and their MF was concentrated in protein binding, cytokine receptor activity, and pattern recognition receptor activity (Fig. 2A). KEGG pathway

analysis showed that these genes were mainly enriched in the cytokine cytokine receptor interaction, HIF-1 signaling pathway, P53 signaling pathway, and MAPK signaling pathway (Fig. 2B, C).

Selection of WGCNA and key modules

We selected genes with expression levels greater than 1 from at least half of the samples to establish a gene set and screened out 11,042 genes. Firstly, we conducted a hierarchical clustering of all sample processes based on the expression levels of all genes. Through this hierarchical clustering, we could check whether there are outliers in the sample, to analyze the sample situation. Then, a gene clustering tree was constructed based on the correlation between gene expression levels, and gene modules were divided based on the clustering relationship between genes. Genes with similar expression patterns would be grouped into the same module, and the branches of the clustering tree would be cut and distinguished to generate different modules, with each color representing one module. The gene co-expression network was divided into 11 gene modules of different colors, with the black module containing a maximum of 2999 genes (Fig. 3).

We used module feature values to perform correlation analysis with specific trait and phenotype data to identify the modules that were most relevant to the trait and phenotype. We selected the module with the highest correlation coefficient GS with HICH, and the darkorange module with a GS of up to 0.69 as the key module. We plotted charts to display the GS and MM, network heatmaps, and expression heatmaps of module genes in different samples in the darkorange module. Among the 559

Table 2 Comparison of baseline characteristics between two groups

Baseline characteristics	HICH group (n = 25)	Control group (n = 22)	χ^2/t	P
Gender[cases (%)]				
Male	16(64.00)	13(59.09)	0.119	0.730
Female	9(36.00)	9(40.91)		
Age ($\bar{x} \pm s$, years old)	69.92 \pm 4.56	68.86 \pm 4.35	0.810	0.422
Smoking history[cases (%)]				
Yes	14(56.00)	11(50.00)	0.169	0.681
No	11(44.00)	11(50.00)		
Systolic pressures ($\bar{x} \pm s$, mmHg)	177.20 \pm 11.08	102.50 \pm 12.53	21.698	< 0.001
Diastolic pressures ($\bar{x} \pm s$, mmHg)	99.60 \pm 12.98	77.50 \pm 8.59	6.781	< 0.001
Diabetes[cases (%)]	13(52.00)	—	—	—
Hyperlipidemia[cases (%)]	11(44.00)	—	—	—
Coronary heart disease[cases (%)]	3(12.00)	—	—	—
Hypertension course ($\bar{x} \pm s$, years)	11.88 \pm 3.06	—	—	—
Cerebral hemorrhage volume ($\bar{x} \pm s$, ml)	47.92 \pm 11.26	—	—	—

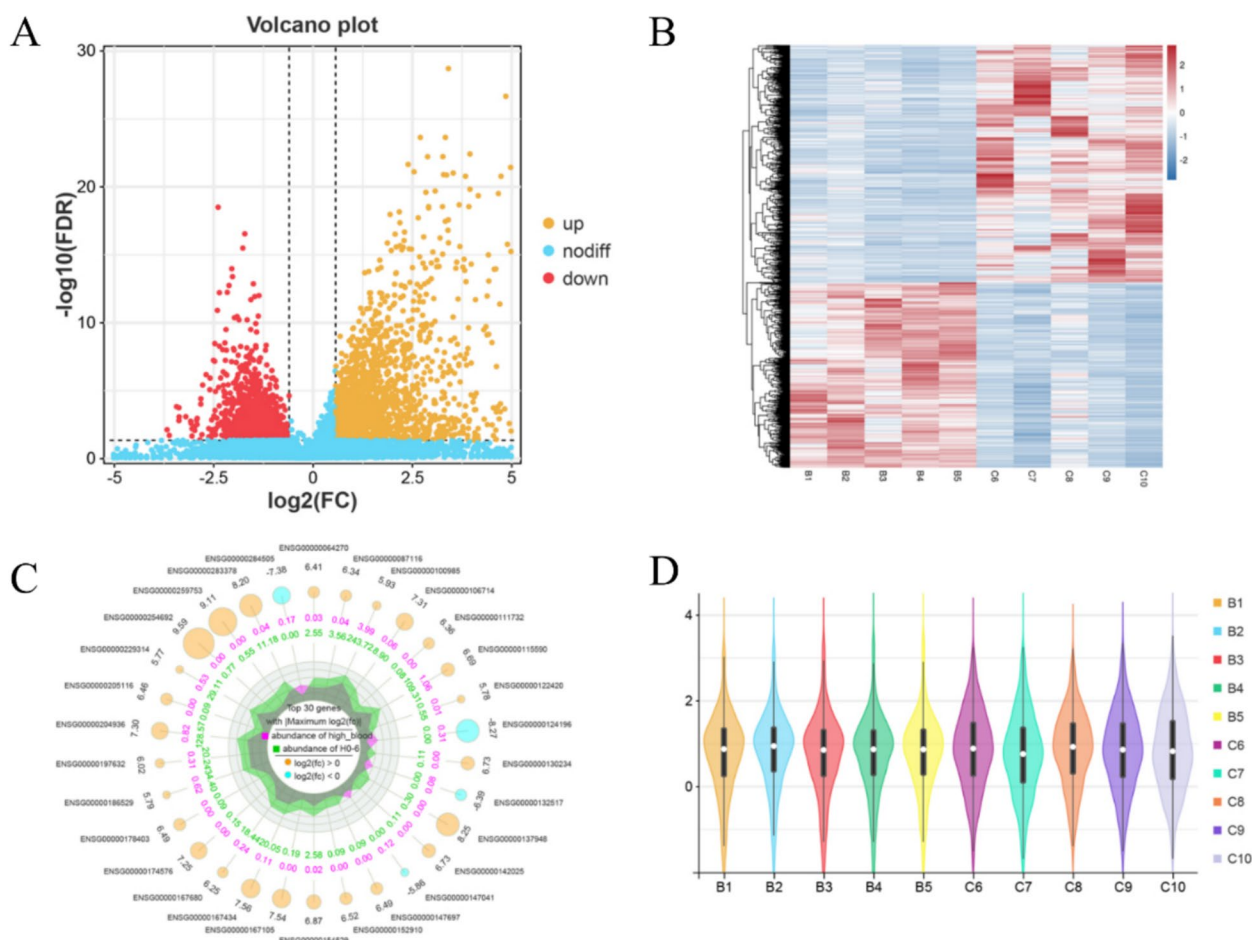


Fig. 1 There are differential expression of genes (DEG) between hypertensive intracerebral hemorrhage group and primary hypertension group. **A** The volcanic map can visually display the differential genes between the comparison groups, with red and yellow dots corresponding to up-regulated and down-regulated mRNAs, and blue dots indicating no difference. **B** Perform hierarchical clustering of differential gene expression patterns and present the clustering results using heat maps. Red represents upregulated genes, while blue represents downregulated genes. **C** The radar map shows the top 30 mRNAs with the highest differential expression between the two groups, with yellow and blue circles representing upregulated and downregulated genes, respectively. The size of the circles varies according to the size of the \log_2 (FC) value. **D** The violin chart displays the data density of differential genes in each sample or group

genes in the darkorange module, 219 central genes with $MM > 0.8$, $GS > 0.5$, and $K_{in} > 50$ were selected (Fig. 4).

GO and KEGG analysis of central genes

We conducted GO and KEGG analysis on the 219 selected central genes. According to GO analysis, the DEGs of cerebral hemorrhage and hypertension were roughly the same. The central genes were also mainly involved in the activation of inflammatory cells and the regulation of immune responses in the BP term. These genes were mainly enriched in the vesicles, cytoplasmic parts, and endometrial system in the CC term, while MF was also concentrated in protein-binding Cytokine receptor activity and pattern recognition receptor activity. KEGG pathway analysis showed that the main pathways

enriched in the central gene include the HIF-1 signaling pathway, chemokine signaling pathway, and VEGF signaling pathway (Fig. 5).

Determine the target mRNA and PPI Network construction

We crossed and intersected the central genes in the key modules with the differentially expressed genes in the hypertensive intracerebral hemorrhage group, resulting in 169 genes. This gene set was designated as the target gene set, and we applied the interaction relationships in the STRING protein interaction database to analyze the differentially expressed gene protein interaction network. We would import the selected target gene set into the STRING website and export the PPI network data to a TSV file. Then we used Cytoscape software to conduct

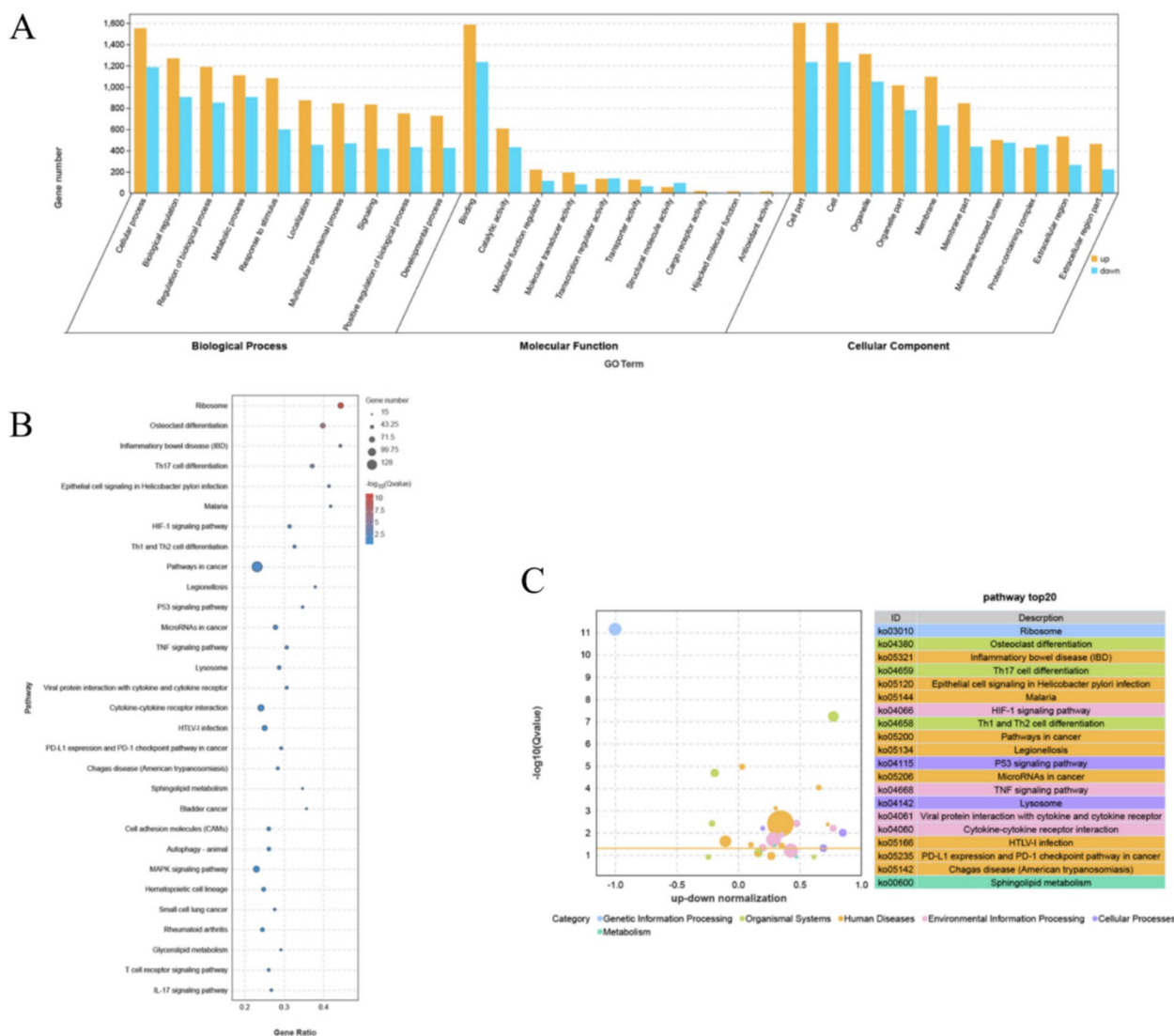


Fig. 2 Results of GO terminology of DEG and KEGG pathway enrichment analysis in the study. **A** The TOP10 items in GO biological process (BP), cell composition (CC), and molecular function (MF) enrichment analysis are sorted by gene enrichment quantity. **B** Bubble chart, selecting significantly enriched Top30 paths based on EDR values. Each bubble represents a path, the size of the bubble represents the number of genes contained in the path, and the color of the bubble represents the significance of the enrichment of the path. **C** Enriched bubble chart, different colors represent different KEGG A class classifications

statistical analysis on the PPI network, screening out the genes that play the main role in the nodes at key hubs in the network and selecting them as our target genes. Finally, we selected 8 target mRNA (SPI1, HK3, HCK, SYK, CD14, FCER1G, CYBB, FGR) (Fig. 6).

Expression distribution and functional analysis of target genes

To specifically investigate the function of the target mRNA, we conducted a KEGG analysis on the target

gene. KEGG analysis showed that SYK and FCER1G mainly participate in the C-type lectin receptor signaling pathway and Fc epsilon RI signaling pathway, CYBB, and HK3 mainly participate in the HIF-1 signaling pathway, FGR and CD14 mainly participate in the chemokine signaling pathway and NF kappa B signaling pathway (Fig. 7). The C-type lectin receptor signaling pathway, Fc epsilon RI signaling pathway, chemokine signaling pathway, and NF kappa B signaling pathway are signaling pathways related to immune inflammatory response.

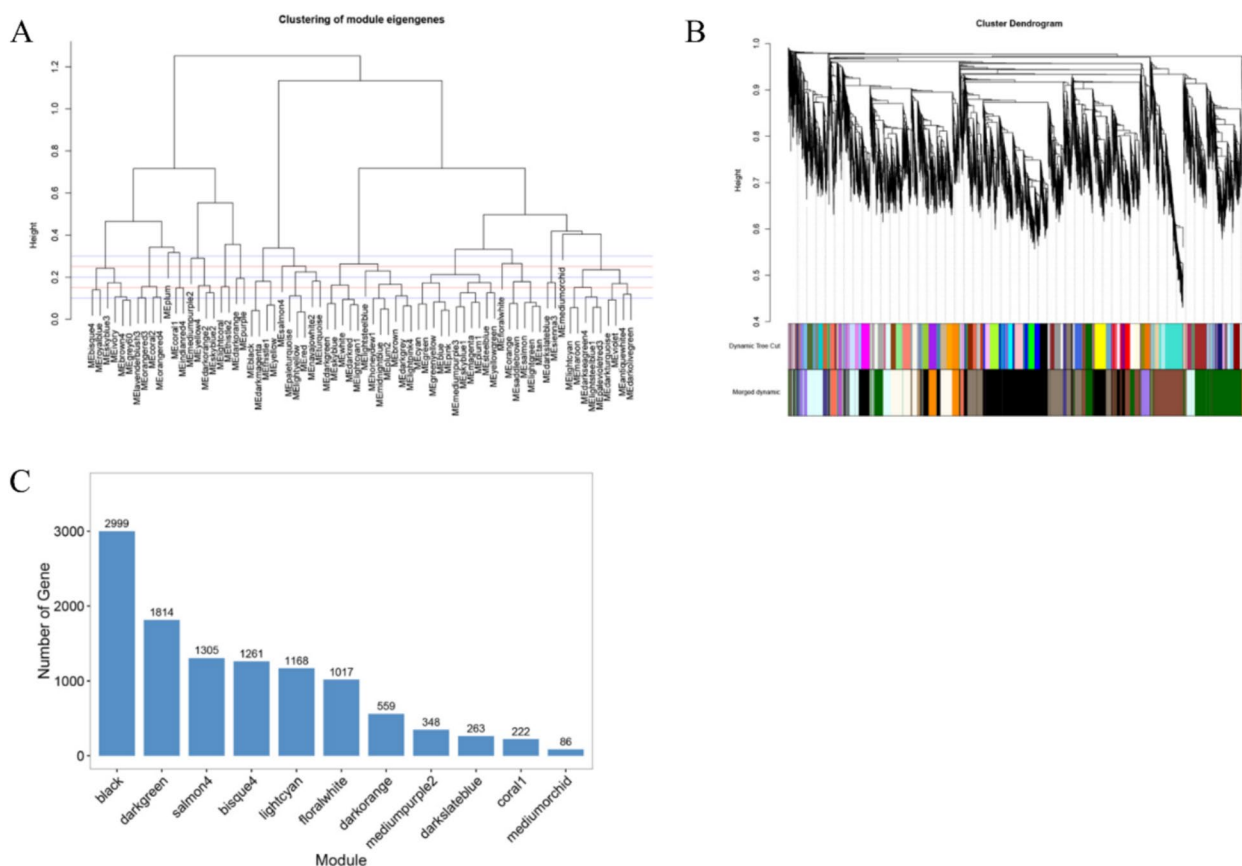


Fig. 3 Construction of Co-expression Network through Weighted Gene Co-expression Network Analysis (WGCNA). **A** Construct gene clustering based on the correlation between gene expression. Each color represents a module, while gray represents genes that cannot be classified into any module. **B** Divide modules based on clustering results. Merge dynamics is the division of modules with similar expression patterns based on their similarity, and subsequent analysis is carried out based on the merged modules. Regarding tree graphs, vertical distance represents the distance between two nodes (genes), while horizontal distance is meaningless. **C** The classification of 11 modules and the number of genes in the modules

Comparison of SPI1, HK3, HCK, SYK, CD14, FCER1G, CYBB and FGR expressions between the two groups

The SPI1, HK3, HCK, SYK, CD14, FCER1G, CYBB and FGR expressions in HICH group were higher than those in the control group ($P < 0.05$), of which SPI1 expression was lower than the control group ($P < 0.05$), as shown in Table 3 and Fig. 8.

Analysis of the relationships between adverse events in the HICH group and mRNA expressions of SPI1, HK3, HCK, SYK, CD14, FCER1G, CYBB, and FGR

In the HICH group, there were 21 cases of pulmonary infection, 4 cases of epilepsy, 5 cases of hematoma enlargement, 12 cases of gastrointestinal bleeding, 21 cases of malnutrition, and 3 cases of lower limb DVT, with incidence rates of 84%, 16%, 20%, 48%, 84%, and 12%, respectively. Age and the expressions of HK3, HCK, SYK, CD14, FCER1G, CYBB, and FGR of patients with pulmonary infection were higher than those without pulmonary infection ($P < 0.05$), as shown in Table 4.

The expression of the SPI1 gene in patients with epilepsy was higher than that in patients without epilepsy ($P < 0.05$), as shown in Table 5.

The expression of SPI1 in patients with hematoma enlargement was lower than that in patients without hematoma enlargement ($P < 0.05$), as shown in Table 6.

The amount of cerebral hemorrhage in patients with gastrointestinal bleeding was higher than that in patients without gastrointestinal bleeding ($P < 0.05$), as shown in Table 7.

Age, HK3, HCK, SYK, CD14, FCER1G, CYBB, and FGR expressions of patients with malnutrition were higher than those of patients without malnutrition ($P < 0.05$), as shown in Table 8.

The expressions of HK3, HCK, SYK, CD14, FCER1G, CYBB, and FGR in patients with lower limb DVT were higher than those in patients without lower limb DVT ($P < 0.05$), as shown in Table 9.

The factors with $P < 0.05$ in the single factor analysis mentioned above were taken as independent variables,

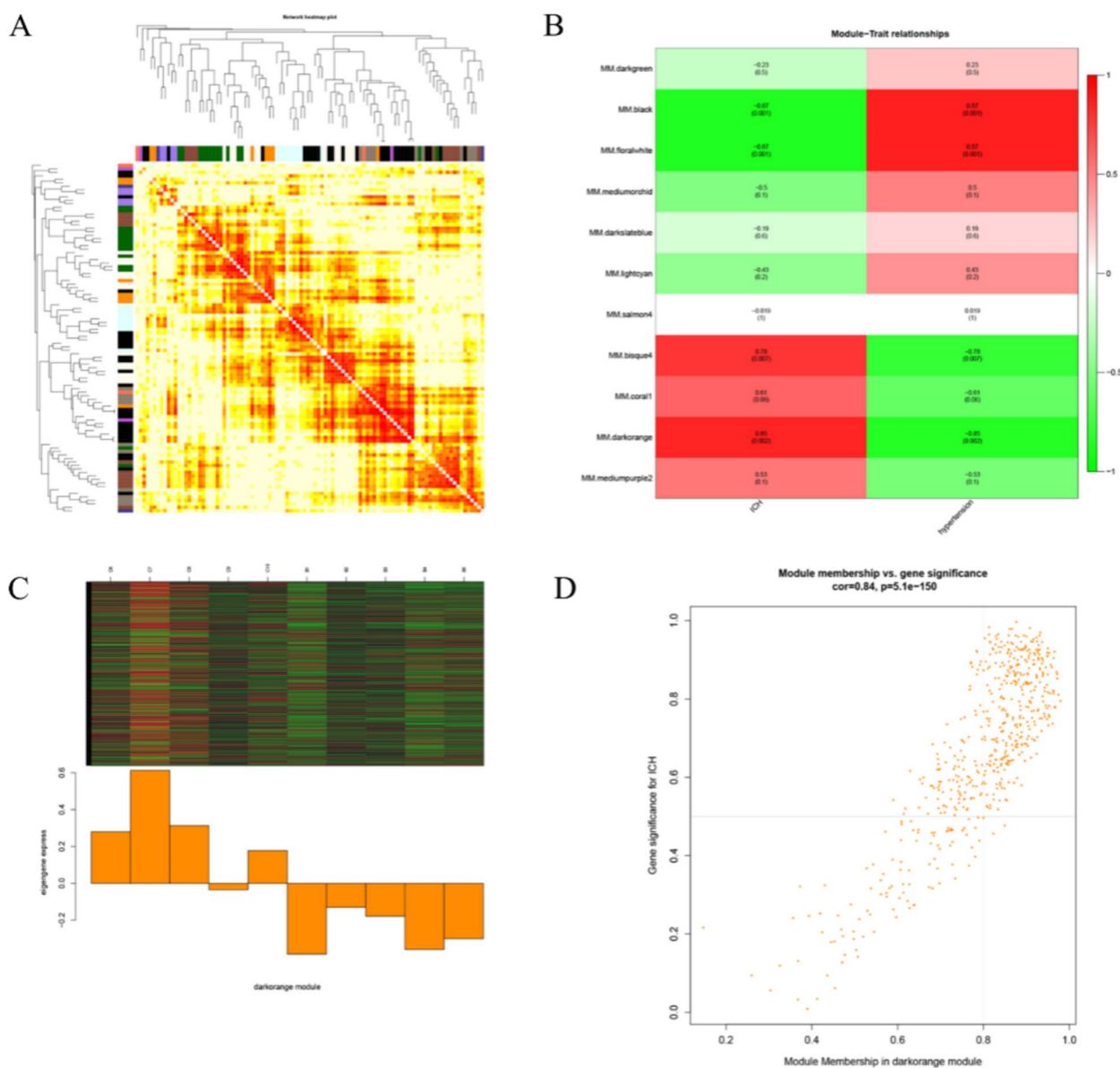


Fig. 4 Selecting key modules and extracting central genes. **A** Module gene correlation heatmap is a correlation analysis of the genes contained in each module. Each row and column represents a gene, and the darker the color of each point (white → yellow → red), the stronger the connectivity between the two genes corresponding to the row and column, that is, the stronger the Pearson correlation. **B** Character correlation graph, with the horizontal axis representing the trait and the vertical axis representing the module, plotted using Pearson correlation coefficients. Red represents a positive correlation, green represents a negative correlation, darker color indicates a stronger correlation, and the number in parentheses below represents the significant *P* value. The smaller the value, the stronger the significance. This graph can intuitively reflect the correlation between each module and each trait. **C** Module gene expression pattern heatmap, the above Fig. shows the expression heatmap of genes in different samples in the module, with red indicating upregulation and green indicating downregulation. **D** Correlation scatter plot, selecting 219 central genes with MM > 0.8, GS > 0.5, and Kin > 50

and the measured values were taken as independent variables for continuous variables. The occurrence of adverse events was taken as the dependent variable, and conditional logistic regression analysis was used. The results showed that age, HCK, SYK, CD14, and

FGR expressions were all influencing factors for lung infection ($P < 0.05$), as shown in Table 10. The analysis results of the influencing factors of other adverse events were shown in Tables 11, 12, 13, 14 and 15, and no possible correlation with gene expression was found ($P > 0.05$).

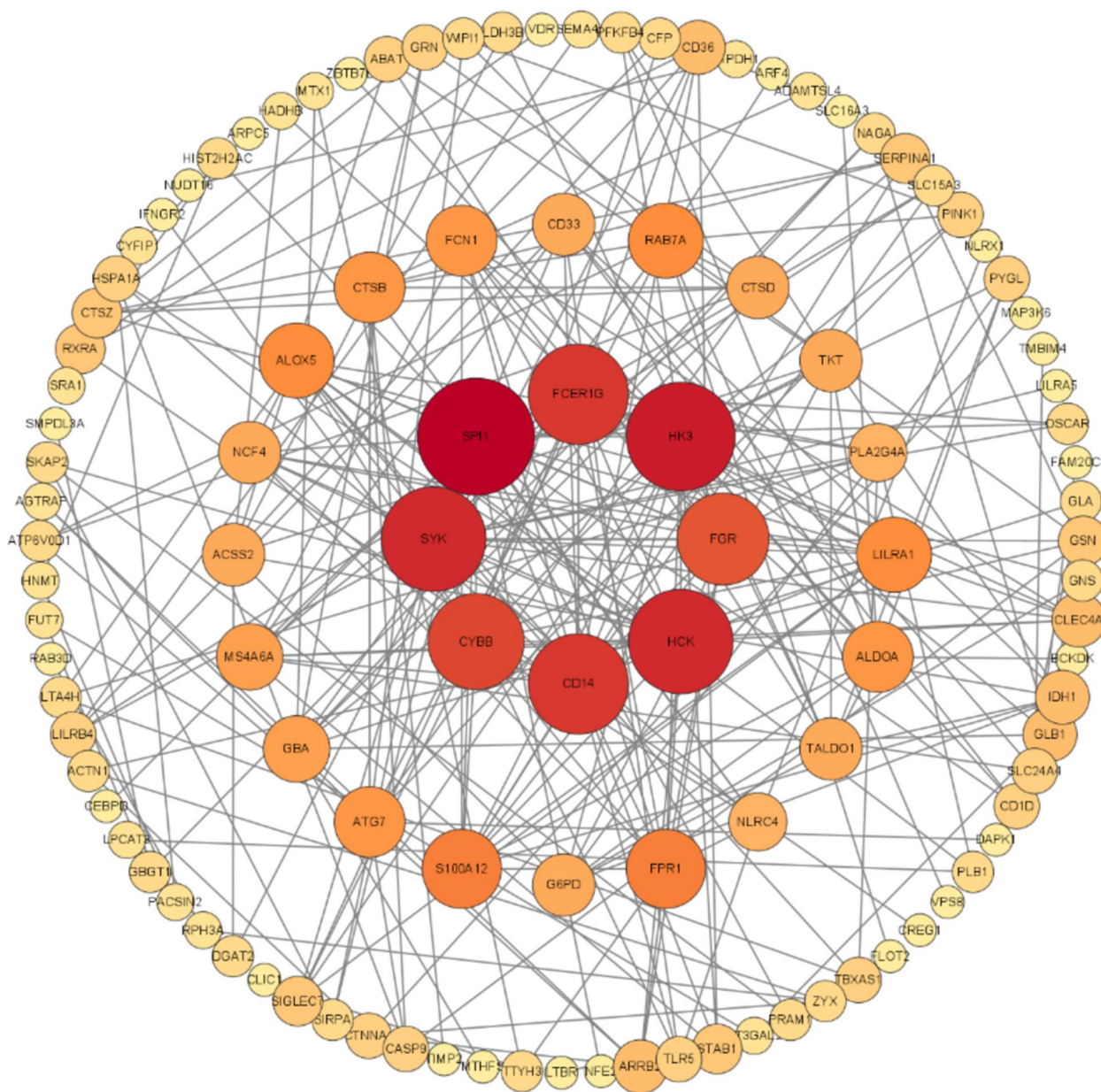


Fig. 6 Protein–Protein Interaction (PPI) Network. Construction of a PPI network consisting of 169 genes in the target gene set. Each circular node represents a gene-encoded protein, the middle red node is a candidate mRNA, and the lines between nodes represent the interactions between proteins

Discussion

The pathophysiological mechanisms of HICH have been a hot topic of research in recent years. Previous experimental studies have found a series of pathological mechanisms after the occurrence of HICH, such as inflammation, neuronal and endothelial cell apoptosis, oxidative stress (OS), etc. [17, 18]. Researchers have been trying to explore the blood mRNA spectrum of ICH. Previously, researchers used high-throughput

sequencing technology to study the mRNA expression profile of patients with cerebral hemorrhage. In differentiated genes, INPP5D (inositol polyphosphatase-5-phosphatase) regulates bone marrow cell proliferation, and ITA4α (integrin) participates in white blood cell recruitment in ICH [19]. In 2019, Stamova studied the use of GeneChip HTA 2.0 arrays in patients with peripheral blood transcriptome cerebral hemorrhage. This study indicates that ICH has differentially expressed T

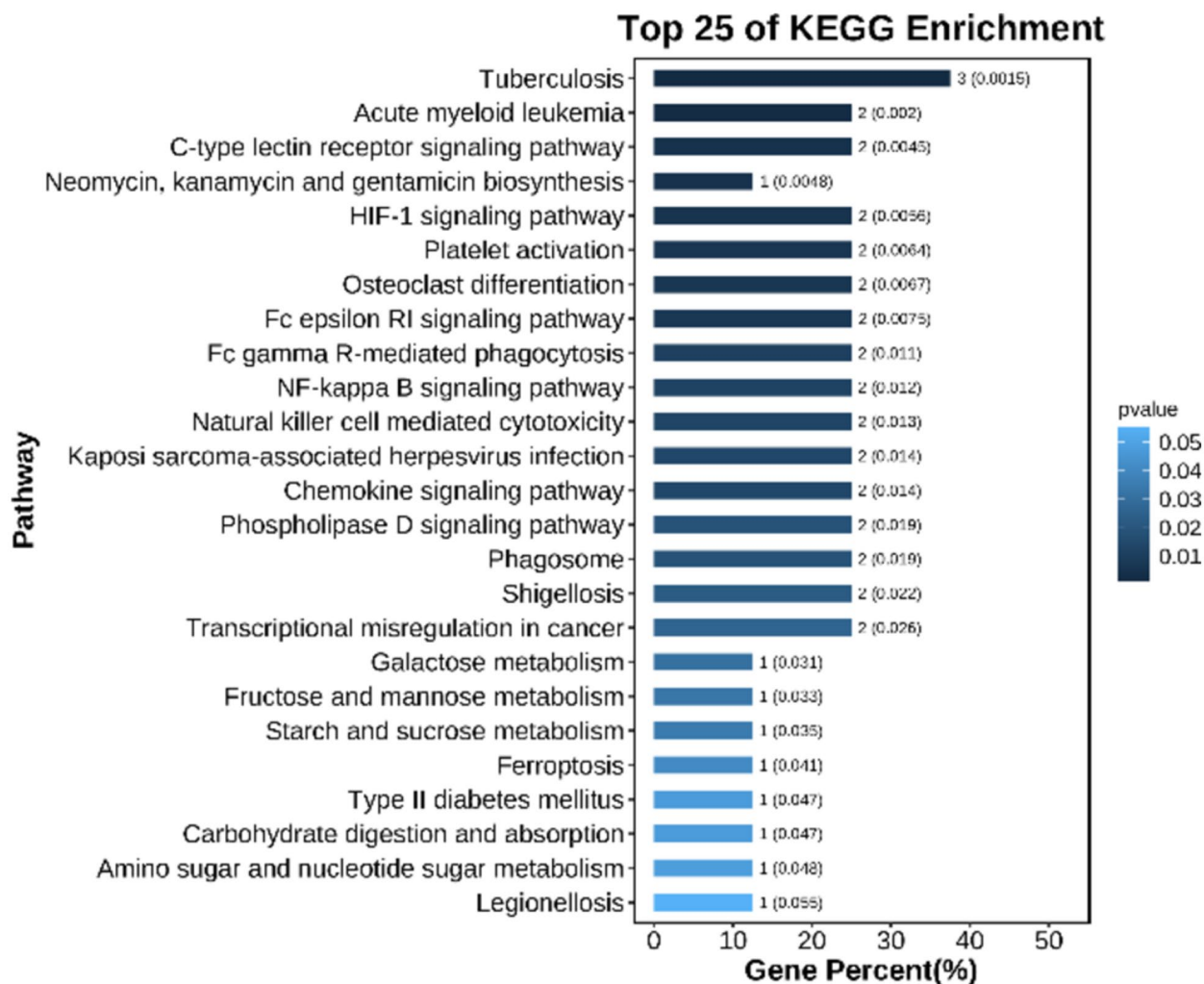


Fig. 7 KEGG bar graph of target genes

cell receptors and CD36 genes, as well as iNOS, TLR, macrophages, and T helper pathways [20]. 250 mRNA changes (136 upregulated and 114 downregulated),

Table 3 Comparison of SPI1, HK3, HCK, SYK, CD14, FCER1G, CYBB and FGR expressions

Genes	HICH group (n=25)	Control group (n=22)	t	P
SPI1	0.64±0.09	1.35±0.09	26.219	<0.001
HK3	1.48±0.25	0.77±0.15	11.594	<0.001
HCK	1.46±0.19	0.61±0.14	17.455	<0.001
SYK	1.48±0.17	0.72±0.12	17.053	<0.001
CD14	1.47±0.19	0.61±0.19	15.729	<0.001
FCER1G	1.67±0.17	0.62±0.14	22.652	<0.001
CYBB	1.43±0.21	0.69±0.10	15.387	<0.001
FGR	1.55±0.19	0.66±0.07	20.778	<0.001

regulating many ICH-related pathways in the whole blood of ICH patients, such as toll-like receptors, natural killer cells, and TGF-β [21].

However, there is limited research on the correlation between brain tissue RNA expression and peripheral blood RNA expression in patients with cerebral hemorrhage. The expression of the GSE24265 gene in brain tissue after intracerebral hemorrhage. Overexpressed genes in the surrounding area of a hematoma encode cytokines, chemokines, coagulation factors, cell growth, and proliferation factors, while low-expressed genes encode proteins related to the cell cycle or neurotrophic factors [22]. In this study, 3163 DEGs were identified in peripheral blood samples of extremely early HICH patients through RNAseq analysis. These DEGs have rich functions in various pathways such as cell death, inflammatory response, and ligand-gated ion channels [23, 24]. Previous reports have suggested that these pathways are associated with

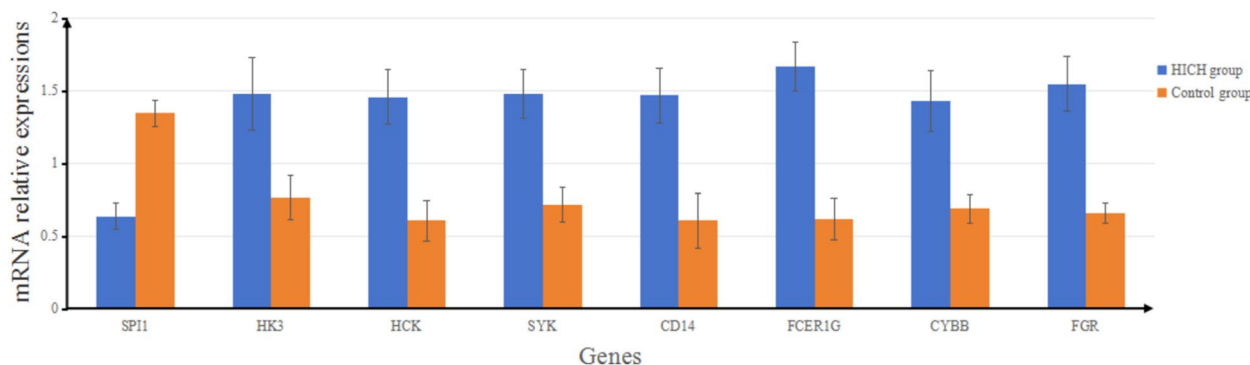


Fig. 8 SPI1, HK3, HCK, SYK, CD14, FCER1G, CYBB and FGR expressions between the two groups

Table 4 Comparison of general information and gene expressions between patients with and without pulmonary infection

General information and gene expressions	With pulmonary infection (n=21)	Without pulmonary infection (n=4)	χ^2/t	P
Gender[cases (%)]				
Male	13(61.90)	3(75.00)	0.250	0.617
Female	8(38.10)	1(25.00)		
Age ($\bar{x} \pm s$, years old)	71.33 \pm 3.18	62.50 \pm 3.42	5.037	<0.001
Smoking history[cases (%)]				
Yes	13(61.90)	1(25.00)	1.857	0.173
No	8(38.10)	3(75.00)		
Systolic pressures ($\bar{x} \pm s$, mmHg)	177.76 \pm 11.66	174.25 \pm 7.80	0.573	0.572
Diastolic pressures ($\bar{x} \pm s$, mmHg)	99.10 \pm 11.52	102.25 \pm 21.27	0.438	0.666
Diabetes[cases (%)]	12(57.14)	1(25.00)	1.391	0.238
Hyperlipidemia[cases (%)]	10(47.62)	1(25.00)	0.698	0.404
Coronary heart disease[cases (%)]	3(14.29)	0(0.00)	0.649	0.420
Hypertension course ($\bar{x} \pm s$, years)	11.86 \pm 3.24	12.00 \pm 2.16	0.084	0.934
Cerebral hemorrhage volume ($\bar{x} \pm s$, ml)	48.38 \pm 11.14	45.50 \pm 13.33	0.461	0.649
Gene expressions				
SPI1	0.63 \pm 0.09	0.66 \pm 0.13	0.502	0.620
HK3	1.54 \pm 0.19	1.17 \pm 0.35	3.093	0.005
HCK	1.51 \pm 0.15	1.21 \pm 0.14	3.581	0.002
SYK	1.52 \pm 0.16	1.28 \pm 0.08	2.872	0.009
CD14	1.53 \pm 0.15	1.19 \pm 0.03	4.434	<0.001
FCER1G	1.71 \pm 0.17	1.49 \pm 0.03	2.581	0.017
CYBB	1.48 \pm 0.18	1.17 \pm 0.08	3.268	0.003
FGR	1.60 \pm 0.16	1.29 \pm 0.10	3.814	0.001

neuronal damage after cerebral hemorrhage. In addition, a total of 11 gene co-expression modules were established through WGCNA. Among them, the darkorange module is the main module related to HICH, containing 559 genes. These genes are enriched in multiple functional pathways such as the HIF-1 signaling pathway, chemokine signaling pathway, and VEGF signaling pathway. Undoubtedly, many researchers have reported that these pathways are involved in the pathogenesis

of cerebral hemorrhage [25, 26]. In addition, there are reports that selective serotonin reuptake inhibitors (SSRIs) have adverse effects on the neurological prognosis of patients with cerebral hemorrhage [27]. Many genes are associated with immune system activation and other inflammatory processes [28]. It is worth mentioning that our study found that the expression of HK3, HCK, SYK, CD14, FCER1G, CYBB, and FGR increased after HICH, while the expression of SPI1 decreased, suggesting that

Table 5 Comparison of general information and gene expressions between patients with and without epilepsy

General information and gene expressions	With epilepsy (n = 4)	Without epilepsy (n = 21)	χ^2/t	P
Gender[cases (%)]				
Male	2(50.00)	14(66.67)	0.405	0.524
Female	2(50.00)	7(33.33)		
Age ($\bar{x} \pm s$, years old)	68.00 \pm 3.56	70.29 \pm 4.71	0.915	0.370
Smoking history[cases (%)]				
Yes	2(50.00)	12(57.14)	0.070	0.792
No	2(50.00)	9(42.86)		
Systolic pressures ($\bar{x} \pm s$, mmHg)	180.00 \pm 6.98	176.67 \pm 11.75	0.554	0.592
Diastolic pressures ($\bar{x} \pm s$, mmHg)	98.25 \pm 12.82	99.86 \pm 13.31	0.222	0.826
Diabetes[cases (%)]	2(50.00)	11(52.38)	0.008	0.930
Hyperlipidemia[cases (%)]	2(50.00)	9(42.86)	0.070	0.792
Coronary heart disease[cases (%)]	0(0.00)	3(14.29)	0.649	0.420
Hypertension course ($\bar{x} \pm s$, years)	11.50 \pm 2.38	11.95 \pm 3.22	0.266	0.793
Cerebral hemorrhage volume ($\bar{x} \pm s$, ml)	54.25 \pm 16.40	46.71 \pm 10.11	1.241	0.227
Gene expressions				
SPI1	0.66 \pm 0.08	0.51 \pm 0.10	3.462	0.002
HK3	1.62 \pm 0.10	1.45 \pm 0.27	1.243	0.226
HCK	1.61 \pm 0.12	1.43 \pm 0.18	1.847	0.078
SYK	1.61 \pm 0.11	1.46 \pm 0.18	1.625	0.118
CD14	1.60 \pm 0.11	1.45 \pm 0.19	1.538	0.138
FCER1G	1.64 \pm 0.17	1.81 \pm 0.10	1.768	0.090
CYBB	1.60 \pm 0.10	1.39 \pm 0.20	1.962	0.062
FGR	1.71 \pm 0.13	1.52 \pm 0.19	1.921	0.067

abnormal expression of these genes may play an important role in the progression of HICH.

HK3 is mainly expressed in hematopoietic cells and tissues and is highly upregulated during the terminal differentiation process of certain acute myeloid leukemia (AML) cell line models. Here, we demonstrate that the expression of HK3 mainly originates from bone marrow cells, and the upregulation of this glycolytic enzyme is not only limited to the differentiation of leukemia cells but also occurs during the in vitro bone marrow differentiation of healthy CD34+ hematopoietic stem cells and progenitor cells. In the hematopoietic system, we found that HK3 is mainly expressed in bone marrow-derived cells. The absence of HK3 can lead to changes in chromatin structure and increase the accessibility of genes involved in cell apoptosis and stress response. HK3 promotes cell survival while also promoting glycolytic activity in AML cells, which is optional [29]. There have been no previous reports on the possible involvement of HK3 in hypertensive intracerebral hemorrhage. However, in the study by Stone JG et al., it was confirmed that HK3 can be expressed in brain tissue, and this protein can participate in cell proliferation, angiogenesis, and vascular damage [30]. Therefore, it is speculated that high expression of HK3 is likely related to cerebrovascular

damage caused by hypertension, thus increasing the risk of intracerebral hemorrhage.

Hematopoietic cell kinase (HCK) is a member of the SRC cytoplasmic tyrosine kinase (SFK) family and is expressed in bone marrow and B lymphocyte lineage cells. HCK enhances the secretion of growth factors and pro-inflammatory cytokines in bone marrow cells, promotes macrophage polarization towards wound healing, and promotes alternate activation phenotypes of tumors. HCK stimulates the formation of podocytes, thereby promoting the degradation of the extracellular matrix and enhancing immune and epithelial cell invasion [31]. HCK can regulate NLRP3 and TGF- β . The signaling pathway is involved in cerebrovascular inflammation, brain cell degeneration, and apoptosis [32, 33]. Currently, no reports are confirming its association with hypertensive intracerebral hemorrhage, and the possible molecular mechanism of HCK involvement in this disease still needs further research. This study also found that HCK is an influencing factor for pulmonary infection in the HICH group. Yamada M et al. showed that bacterial pneumonia mice can secrete interferon, and HCK can regulate the Fgr/Lyn pathway to affect interferon secretion [34]; Zhang X et al. also found that HCK is highly expressed in children with sepsis, which is closely related

Table 6 Comparison of general information and gene expressions between patients with and without hematoma enlargement

General information and gene expressions	With hematoma enlargement (n = 5)	Without hematoma enlargement (n = 20)	χ^2/t	P
Gender[cases (%)]				
Male	3(60.00)	13(65.00)	0.043	0.835
Female	2(40.00)	7(35.00)		
Age ($\bar{x} \pm s$, years old)	67.20 \pm 3.56	70.60 \pm 4.60	1.531	0.139
Smoking history[cases (%)]				
Yes	3(60.00)	11(55.00)	0.041	0.840
No	2(40.00)	9(45.00)		
Systolic pressures ($\bar{x} \pm s$, mmHg)	180.20 \pm 6.06	176.45 \pm 12.01	0.669	0.510
Diastolic pressures ($\bar{x} \pm s$, mmHg)	105.40 \pm 19.46	98.15 \pm 11.04	1.123	0.273
Diabetes[cases (%)]	2(40.00)	11(55.00)	0.361	0.548
Hyperlipidemia[cases (%)]	2(40.00)	9(45.00)	0.041	0.840
Coronary heart disease[cases (%)]	0(0.00)	3(15.00)	0.852	0.356
Hypertension course ($\bar{x} \pm s$, years)	11.20 \pm 2.17	12.05 \pm 3.27	0.547	0.586
Cerebral hemorrhage volume ($\bar{x} \pm s$, ml)	56.40 \pm 14.99	45.80 \pm 9.44	1.997	0.058
Gene expressions				
SPI1	0.51 \pm 0.01	0.67 \pm 0.08	4.241	< 0.001
HK3	1.54 \pm 0.19	1.46 \pm 0.27	0.649	0.523
HCK	1.52 \pm 0.23	1.45 \pm 0.18	0.795	0.435
SYK	1.53 \pm 0.20	1.47 \pm 0.17	0.685	0.500
CD14	1.52 \pm 0.20	1.46 \pm 0.18	0.628	0.536
FCER1G	1.74 \pm 0.17	1.65 \pm 0.17	1.007	0.325
CYBB	1.51 \pm 0.22	1.41 \pm 0.20	1.001	0.327
FGR	1.61 \pm 0.25	1.54 \pm 0.18	0.786	0.440

to bacterial infection [35]. This study is consistent with the above analysis, which suggests that high expression of HCK is involved in the synthesis and secretion of pro-inflammatory factors, enhances pro-inflammatory factor activity, and thus increases the risk of pulmonary infection in hypertensive intracerebral hemorrhage.

Spleen tyrosine kinase (SYK) is a 72 kDa cytoplasmic non receptor tyrosine kinase and is a member of the SRC family. It is widely expressed in various cell types, including hematopoietic cells (such as B cells, immature T cells, neutrophils, mast cells, macrophages, and platelets) and non-hematopoietic cells (epithelial cells, fibroblasts, ACCESSSED MANUSCRIPT neurons, vascular endothelial cells, liver cells, and osteoclasts), promoting various downstream signaling pathways and mediating different biological functions. Active SYK is widely involved in the transduction of various downstream signaling pathways, such as PI3K-AKT, Ras-ERK, PLC γ - NFAT, Vav1 Rac, and NF κ B pathway [36]. Liu XY et al. showed that acupuncture at Baihui and Qubin points after cerebral hematoma can alleviate neurological dysfunction, and the mechanism of action is related to the inhibition of the macroscopic inducible C-type lectin/spleen tyrosine kinase (Mincle/SYK) pathway [37]. Xie Y et al. found

that inhibiting the Mincle/SYK pathway can alleviate glial inflammatory response, alleviate early vascular and neurological dysfunction in rats with subarachnoid hemorrhage, and have a positive effect on inhibiting intravascular perforation [38]. Based on the combination of this study and the above analysis, it is speculated that high expression of SYK can induce inflammatory response damage to cerebral vasculature, promote intravascular perforation, and cause cerebral hemorrhage. This study also found that high expression of SYK is a contributing factor to lung infection, and studies have found that SYK is a biomarker for lung diseases and *Pseudomonas aeruginosa* infection [39, 40]; There are also reports suggesting that CYK can inhibit the body's immune system and promote the replication of influenza A virus in the later stage of virus infection [41]. Therefore, the increased expression of SYK is related to both pulmonary bacterial and viral infections.

Human monocyte differentiation antigen CD14 is a pattern recognition receptor (PRR) that enhances innate immune response. In addition to its role in innate immunity, CD14 is considered to have a more general role in regulating cancer, atherosclerosis, metabolic diseases, etc. In addition, CD14 is involved in regulating

Table 7 Comparison of general information and gene expressions between patients with and without gastrointestinal bleeding

General information and gene expressions	With gastrointestinal bleeding (n = 12)	Without gastrointestinal bleeding (n = 13)	χ^2/t	P
Gender[cases (%)]				
Male	8(66.67)	8(61.54)	0.071	0.790
Female	4(33.33)	5(38.46)		
Age ($\bar{x} \pm s$, years old)	69.17 \pm 5.42	70.62 \pm 3.69	0.787	0.440
Smoking history[cases (%)]			1.629	0.117
Yes	5(41.67)	6(46.15)	0.051	0.821
No	7(58.33)	7(53.85)		
Systolic pressures ($\bar{x} \pm s$, mmHg)	180.83 \pm 8.10	173.85 \pm 12.64	1.629	0.117
Diastolic pressures ($\bar{x} \pm s$, mmHg)	101.00 \pm 14.08	98.31 \pm 12.30	0.510	0.615
Diabetes[cases (%)]	8(66.67)	5(38.46)	1.989	0.158
Hyperlipidemia[cases (%)]	5(41.67)	6(46.15)	0.051	0.821
Coronary heart disease[cases (%)]	1(8.33)	2(15.38)	0.294	0.588
Hypertension course ($\bar{x} \pm s$, years)	11.33 \pm 2.74	12.38 \pm 3.36	0.853	0.402
Cerebral hemorrhage volume ($\bar{x} \pm s$, ml)	53.38 \pm 10.34	42.00 \pm 9.29	2.886	0.008
Gene expressions				
SPI1	0.64 \pm 0.11	0.63 \pm 0.08	0.263	0.795
HK3	1.47 \pm 0.30	1.49 \pm 0.22	0.188	0.852
HCK	1.44 \pm 0.23	1.48 \pm 0.14	0.527	0.603
SYK	1.49 \pm 0.19	1.47 \pm 0.16	0.271	0.789
CD14	1.46 \pm 0.21	1.49 \pm 0.17	0.389	0.701
FCER1G	1.69 \pm 0.20	1.65 \pm 0.16	0.521	0.607
CYBB	1.44 \pm 0.23	1.41 \pm 0.19	0.322	0.750
FGR	1.55 \pm 0.23	1.56 \pm 0.16	0.091	0.928

insulin action and adipogenesis. FCER1G is a key molecule involved in allergic reactions, located on chromosome 1q23.3 and encoding the immunoglobulin fragment crystallization (Fc) region (Fc R) γ Subunits [42]. FCER1G is involved in many diseases, such as squamous cell carcinoma, diabetes nephropathy, multiple myeloma, and clear cell renal cell carcinoma [43]. CYBB in cDCs enhances myelin-specific CD4+ T cell activation through antigen presentation, allows CNS immune invasion, and promotes TH cell-mediated tissue damage during AT-EAE. CYBB-mediated ROS production can be detected in many hematopoietic and non-hematopoietic cell lineages, such as fibroblasts, endothelial cells, and myocardial cells. FGR mediates the induction of fibrosis by aging cells [44]. FGR kinase is associated with pro-inflammatory adipose tissue macrophage activation, diet-induced obesity, insulin resistance, and liver steatosis [45]. FGR deficiency is associated with reduced secretion of chemokines in the lungs in response to lipopolysaccharides. Girard R et al. found that CD14 belongs to the biomarker of inflammatory response, which can mediate the damage of inflammatory response to brain tissue after cerebral hemorrhage [46]. However, the mechanism by which CD14 participates in the occurrence of

hypertensive cerebral hemorrhage is still unclear. Elias Oliveira J et al. pointed out that xylose oxidase-induced CD14 deficient mice had smaller lung tissue damage areas, less infiltration of neutrophils and macrophages, and milder pulmonary edema [47]. This study also found that high expression of CD14 is a risk factor for pulmonary infection in hypertensive intracerebral hemorrhage. It is speculated that high expression of CD14 is associated with more inflammatory cell infiltration and more severe pulmonary edema.

FCER1G belongs to the immunoglobulin superfamily and plays an important role in immune system defense. Fc receptors are present on the surfaces of B lymphocytes, macrophages, natural killer cells, and other cells. When these receptors are lacking, the immune function of these cells will be impaired, which can cause cellular immune disorders. Correspondingly, the expression of FCER1G can also participate in the regulation of cellular immune function. Some studies suggest that FCER1G is a key gene in renal clear cell carcinoma, and the occurrence of cancer is closely related to immune escape [48]. Some studies found that the high expression of FCER1G may induce acute cerebral infarction by promoting atherosclerosis [49]. However, there are currently no reports

Table 8 Comparison of general information and gene expressions between patients with and without malnutrition

General information and gene expressions	With malnutrition (n=21)	Without malnutrition (n=4)	χ^2/t	P
Gender[cases (%)]				
Male	13(61.90)	3(75.00)	0.250	0.617
Female	8(38.10)	1(25.00)		
Age ($\bar{x} \pm s$, years old)	70.95 \pm 3.32	64.50 \pm 6.81	2.990	0.007
Smoking history[cases (%)]				
Yes	13(61.90)	1(25.00)	1.857	0.173
No	8(38.10)	3(75.00)		
Systolic pressures ($\bar{x} \pm s$, mmHg)	178.05 \pm 11.56	172.75 \pm 7.68	0.872	0.392
Diastolic pressures ($\bar{x} \pm s$, mmHg)	98.29 \pm 11.23	106.50 \pm 20.76	1.169	0.254
Diabetes[cases (%)]	11(52.38)	2(50.00)	0.008	0.930
Hyperlipidemia[cases (%)]	9(42.86)	2(50.00)	0.070	0.792
Coronary heart disease[cases (%)]	3(14.29)	0(0.00)	0.649	0.420
Hypertension course ($\bar{x} \pm s$, years)	11.57 \pm 2.93	13.50 \pm 3.70	1.164	0.256
Cerebral hemorrhage volume ($\bar{x} \pm s$, ml)	48.05 \pm 11.44	47.25 \pm 11.87	0.127	0.900
Gene expressions				
SPI1	0.63 \pm 0.09	0.65 \pm 0.12	0.329	0.745
HK3	1.52 \pm 0.20	1.23 \pm 0.39	2.325	0.029
HCK	1.52 \pm 0.14	1.16 \pm 0.04	4.947	< 0.001
SYK	1.52 \pm 0.17	1.31 \pm 0.11	2.417	0.025
CD14	1.52 \pm 0.16	1.23 \pm 0.11	3.387	0.003
FCER1G	1.71 \pm 0.15	1.44 \pm 0.07	3.556	0.002
CYBB	1.47 \pm 0.19	1.20 \pm 0.12	2.676	0.013
FGR	1.59 \pm 0.17	1.33 \pm 0.15	2.893	0.008

on the mechanism of this gene participating in hypertensive intracerebral hemorrhage both domestically and internationally, suggesting that it may be related to immune inflammatory response.

CYBB is one of the subunits of NADPH oxidase, which is an X-linked recessive inheritance. It is a common genetic factor in immune deficiency and is also related to genetic defects in phagocytes. According to previous reports, CYBB can participate in the occurrence of non-alcoholic steatohepatitis and the formation of liver tumors [50]. There is also a report confirming that CYBB can regulate the antigen processing of myelin oligodendrocytes in dendritic cells, leading to the initiation and maintenance of autoimmune neuroinflammation by brain T helper cells [44]. Additionally, CYBB gene ablation can inhibit the recruitment of T helper cells from encephalitis to central nervous cells. Although there have been no previous reports of high expression of CYBB and hypertensive intracerebral hemorrhage, it is evident that CYBB participates in neuroinflammatory damage through multiple molecular pathways.

FGR is a homolog of the oncogenic gene of the feline sarcoma virus and a member of the Scr protein tyrosine kinase family. The protein encoded by FGR is β - Two

important molecules in the signaling pathway of integrin 2 can trigger negative feedback regulation of cell migration and adhesion. High expression in tumor cells can inhibit their migration and invasion activities. Gut-kind JS et al. pointed out that FGR expression is related to neutrophil activation [51]. However, further research is needed on how FGR participates in the occurrence of hypertensive intracerebral hemorrhage. This study also found that FGR expression is a risk factor for lung infection. Nelson MP et al. found that knocking out FGR inhibits its tyrosine kinase activity and enhances the immune response of lung tissue to pulmonary sporidiosis [52]. Another study has confirmed that inhibiting the expression of FGR can induce alveolar macrophages to enhance their defense against atypical pneumocystis [53]. From this, it can be inferred that high expression of FGR may lead to pulmonary infection in patients with hypertensive intracerebral hemorrhage by reducing the defense effect of lung tissue against pathogenic microbial invasion.

SPI1 is a transcription factor that encodes the ETS domain and regulates gene expression during the development of myeloid cells and B lymphocytes. SPI1 is a key transcription factor after intracerebral hemorrhage,

Table 9 Comparison of general information and gene expressions between patients with and without lower-limb DVT

General information and gene expressions	With lower limb DVT (n = 3)	Without lower limb DVT (n = 22)	χ^2/t	P
Gender[cases (%)]				
Male	2(66.67)	14(63.64)	0.011	0.918
Female	1(33.33)	8(36.36)		
Age ($\bar{x} \pm s$, years old)	69.00 \pm 3.00	70.05 \pm 4.78	0.365	0.718
Smoking history[cases (%)]				
Yes	2(66.67)	12(54.55)	0.157	0.692
No	1(33.33)	10(45.45)		
Systolic pressures ($\bar{x} \pm s$, mmHg)	188.67 \pm 4.04	175.64 \pm 10.83	2.032	0.054
Diastolic pressures ($\bar{x} \pm s$, mmHg)	103.00 \pm 6.08	99.14 \pm 13.68	0.476	0.639
Diabetes[cases (%)]	2(66.67)	11(50.00)	0.294	0.588
Hyperlipidemia[cases (%)]	1(33.33)	10(45.45)	0.157	0.692
Coronary heart disease[cases (%)]	0(0.00)	3(13.64)	0.465	0.495
Hypertension course ($\bar{x} \pm s$, years)	11.67 \pm 2.08	11.91 \pm 3.21	0.126	0.901
Cerebral hemorrhage volume ($\bar{x} \pm s$, ml)	41.67 \pm 9.07	48.77 \pm 11.43	1.027	0.315
Gene expressions				
SPI1	0.66 \pm 0.12	0.63 \pm 0.09	0.408	0.687
HK3	1.78 \pm 0.07	1.44 \pm 0.24	2.422	0.024
HCK	1.76 \pm 0.10	1.42 \pm 0.16	3.623	0.001
SYK	1.76 \pm 0.02	1.44 \pm 0.15	3.668	0.001
CD14	1.71 \pm 0.02	1.44 \pm 0.17	2.589	0.016
FCER1G	1.97 \pm 0.08	1.63 \pm 0.14	4.185	< 0.001
CYBB	1.72 \pm 0.03	1.39 \pm 0.19	3.042	0.006
FGR	1.81 \pm 0.08	1.52 \pm 0.17	2.871	0.009

Table 10 Logistic regression analysis of influencing factors of pulmonary infection

Factors	B	S.E	Wals	P	OR	95%CI (Down)	95%CI (Up)
Age	2.488	0.744	11.183	< 0.001	12.035	2.800	51.740
HK3	51.893	145,205.300	< 0.001	1.000	3.443	< 0.001	
HCK	2.127	0.781	7.417	0.001	8.390	1.815	38.774
SYK	1.655	0.563	8.641	< 0.001	5.232	1.736	15.776
CD14	2.375	0.821	8.368	< 0.001	10.751	2.151	53.740
FCER1G	82.942	228,720.280	< 0.001	1.000	1.050E + 36	< 0.001	
CYBB	-117.113	620,789.660	< 0.001	1.000	< 0.001	< 0.001	
FGR	1.982	0.436	20.665	< 0.001	7.257	3.088	17.057
Constant term	-451.381	902,431.444	< 0.001	1.000	< 0.001		

Table 11 Logistic regression analysis of the influencing factors of epilepsy

Factors	B	S.E	Wals	P	OR	95%CI (Down)	95%CI (Up)
SPI1	-1330.401	109506.100	< 0.001	0.990	< 0.001	< 0.001	
Constant term	692.502	56943.170	< 0.001	0.990	5.620E300		

Table 12 Logistic regression analysis of influencing factors of hematoma enlargement

Factors	B	S.E	Wals	P	OR	95%CI (Down)	95%CI (Up)
SPI1	-1540.296	119177.021	<0.001	0.990	<0.001	<0.001	
Constant term	817.015	63303.851	<0.001	0.990			

Table 13 Logistic regression analysis of influencing factors of gastrointestinal bleeding

Factors	B	S.E	Wals	P	OR	95%CI (Down)	95%CI (Up)
Cerebral hemorrhage volume	1.196	4.371	0.075	0.784	3.308	0.001	17388.528
Constant term	-0.841	2.809	0.090	0.765	0.431		

Table 14 Logistic regression analysis of influencing factors of malnutrition

Factors	B	S.E	Wals	P	OR	95%CI (Down)	95%CI (Up)
Age	2.911	2482.660	<0.001	0.999	18.381	<0.001	
HK3	5.526	174923.313	<0.001	1.000	251.190	<0.001	
HCK	101.357	96063.595	<0.001	0.999	1.044E44	<0.001	
SYK	64.846	392516.776	<0.001	1.000	1.453E28	<0.001	
CD14	-109.095	146315.704	<0.001	0.999	<0.001	<0.001	
FCER1G	131.746	94078.636	<0.001	0.999	1.646E57	<0.001	
CYBB	-95.616	445484.449	<0.001	1.000	<0.001	<0.001	
FGR	39.865	127040.476	<0.001	1.000	2.057E17	<0.001	
Constant term	-412.034	166533.242	<0.001	0.998	<0.001		

Table 15 Logistic regression analysis of influencing factors of lower limb DVT

Factors	B	S.E	Wals	P	OR	95%CI (Down)	95%CI (Up)
HK3	50.248	205060.931	<0.001	1.000	6.644E21	<0.001	
HCK	-15.512	756038.569	<0.001	1.000	<0.001	<0.001	
SYK	413.079	413591.625	<0.001	0.999	2.499E179	<0.001	
CD14	-280.577	437350.431	<0.001	0.999	<0.001	<0.001	
FCER1G	91.116	156215.880	<0.001	1.000	3.725E39	<0.001	
CYBB	-107.311	90886.604	<0.001	0.999	<0.001	<0.001	
FGR	44.442	96877.561	<0.001	1.000	1.999E19	<0.001	
Constant term	-358.466	191116.872	<0.001	0.999	<0.001		

and its expression is significantly increased after intracerebral hemorrhage. In the study by Zhang G et al., SPI1 expression was significantly increased after cerebral hemorrhage [54]. SPI1 can regulate the transcriptome expression of brain microglia, enhance their phagocytosis, and is related to glycolysis, autophagy of brain cells, and myelin regeneration. Further research suggests that SPI1 may continue to participate in FCGR1, affecting central nervous system function. In this study,

the expression of SPI1 in patients with hypertensive intracerebral hemorrhage significantly decreased, which is inconsistent with the above reports. It may be related to different designed primer sequences, different sample detection time points, differences in detection equipment sensitivity, and differences in patient sources. However, our research team also found that SPI1 is highly expressed in some patients with hypertensive intracerebral hemorrhage in the early stage, and

gradually decreases thereafter. This suggests that SPI1 is dynamically changing during the occurrence and development of hypertensive intracerebral hemorrhage, and the reasons for this rapid and significant change are still unknown.

In this study, it was found that the expression of HK3, HCK, SYK, CD14, FCER1G, CYBB, and FGR in hypertensive intracerebral hemorrhage was higher than that in the control group, while the expression of SPI1 was lower than that in the control group. However, the above gene testing results of some patients did not conform to this trend, which may be related to differences in underlying diseases and individual health levels. However, this individual difference does not affect the progress of the study. In addition, although this study found that there may be statistical differences in the genes mentioned above between patients with epilepsy, enlarged hematoma, gastrointestinal bleeding, malnutrition, and lower limb DVT compared to those who did not, it was not found that these genes may affect adverse events, which may be due to the small sample size of the study leading to biased results.

The sample size of this study is small, and there are some errors. The innovation points of our research are difficult to summarize from the perspective of computer and contribute from the perspective of application, but there are contradictions in the contribution points of the paper, and the knowledge update iteration is fast and requires continuous learning. Early HICH data are also being updated. We will monitor the data and release the latest research results in a timely manner.

Conclusion

This study screened candidate genes for hypertensive intracerebral hemorrhage, including SPI1, HK3, HCK, SYK, CD14, FCER1G, CYBB, FGR, which can participate in the HIF-1 signaling pathway, NF-kappa B signaling pathway, and C-type lectin receptor signaling pathway. These genes may affect the development of hypertensive intracerebral hemorrhage through cell apoptosis, immune response, and inflammatory response. In patients with hypertensive intracerebral hemorrhage, the expressions of HK3, HCK, SYK, CD14, FCER1G, CYBB, and FGR increase, while the expression of SPI1 decreases. Age, HCK, SYK, CD14, and FGR expressions are all influencing factors for the occurrence of pulmonary infection in patients.

Acknowledgements

The Henan Provincial Department of Science and Technology provided research funding. The Fifth Affiliated Hospital of Zhengzhou University provided participants. The Central Laboratory of Zhengzhou University Fifth Affiliated Hospital and the Brain Glioma Microecology Laboratory provided experimental conditions.

Authors' contributions

Gao Hai-dong, Shou Ji-xin and Wang Jian-ye brewed and designed experiments. Zhang Jian, Cheng Sen, Guan Hai-bo, Wang Bing-bing, Zhou Shao-long, Ding Pan-feng and Yang Peng conducted research and collected data. Liang Wu-long and Lv Yuan analyzed/interpreted data. Gao Hai-dong drafted this article. Wang Xin-jun's critical review, statistical analysis, and supportive contribution to the knowledge-based content of the article.

Funding

Henan Provincial Department of Science and Technology Science and Technology Research Program Project (Project Number: 222102310620).

Data availability

No datasets were generated or analysed during the current study.

Declarations

Ethics approval and consent to participate

This study was conducted in accordance with the Declaration of Helsinki and approved by the Ethics Committee of Zhengzhou University Fifth Affiliated Hospital (Y2021052).

Consent for publication

All authors agree to submit and publish.

Competing interests

The authors declare no competing interests.

Author details

¹Department of Neurosurgery, Zhengzhou University Fifth Affiliated Hospital, Erqi District, No.3, Rehabilitation Front Street, Zhengzhou, Henan 45000, China.

Received: 19 September 2024 Accepted: 22 November 2024

Published online: 30 November 2024

References

- Hawkes MA, Rabinstein AA. Acute Hypertensive Response in Patients With Acute Intracerebral Hemorrhage: A Narrative Review. *Neurology*. 2021;97(7):316–29.
- Global, regional, and national burden of stroke, 1990–2016: a systematic analysis for the Global Burden of Disease Study 2016. *Lancet Neurol*. 2019;18(5): 439–458.
- Takada S, Sakakima H, Matsuyama T, et al. Disruption of Midkine gene reduces traumatic brain injury through the modulation of neuroinflammation. *J Neuroinflammation*. 2020;17(1):40.
- Aronowski J, Zhao X. Molecular pathophysiology of cerebral hemorrhage: secondary brain injury. *Stroke*. 2011;42(6):1781–6.
- Troiani Z, Ascanio L, Rossitto CP, et al. Prognostic Utility of Serum Biomarkers in Intracerebral Hemorrhage: A Systematic Review. *Neurorehabil Neural Repair*. 2021;35(11):946–59.
- Jin F, Li L, Hao Y, Tang L, Wang Y, He Z. Identification of Candidate Blood mRNA Biomarkers in Intracerebral Hemorrhage Using Integrated Microarray and Weighted Gene Co-expression Network Analysis. *Front Genet*. 2021;12: 707713.
- Yang T, Gu J, Kong B, et al. Gene expression profiles of patients with cerebral hematoma following spontaneous intracerebral hemorrhage. *Mol Med Rep*. 2014;10(4):1671–8.
- Chen B, Sun H, Zhao Y, Lun P, Feng Y. An 85-Genes Coexpression Module for Progression of Hypertension-Induced Spontaneous Intracerebral Hemorrhage. *DNA Cell Biol*. 2019;38(5):449–56.
- Zhang B, Horvath S. A general framework for weighted gene co-expression network analysis. *Stat Appl Genet Mol Biol*. 2005;4: Article17.
- Ashburner M, Ball CA, Blake JA, et al. Gene ontology: tool for the unification of biology. *The Gene Ontology Consortium Nat Genet*. 2000;25(1):25–9.
- Kanehisa M, Goto S. KEGG: kyoto encyclopedia of genes and genomes. *Nucleic Acids Res*. 2000;28(1):27–30.

12. Subramanian A, Tamayo P, Mootha VK, et al. Gene set enrichment analysis: a knowledge-based approach for interpreting genome-wide expression profiles. *Proc Natl Acad Sci U S A*. 2005;102(43):15545–50.
13. Love MI, Huber W, Anders S. Moderated estimation of fold change and dispersion for RNA-seq data with DESeq2. *Genome Biol*. 2014;15(12):550.
14. Wang W, Zhang F, Cui J, et al. Identification of microRNA-like RNAs from *Trichoderma asperellum* DQ-1 during its interaction with tomato roots using bioinformatic analysis and high-throughput sequencing. *PLoS One*. 2021;16(7):e0254808.
15. Langfelder P, Horvath S. WGCNA: an R package for weighted correlation network analysis. *BMC Bioinformatics*. 2008;9:559.
16. Shannon P, Markiel A, Ozier O, et al. Cytoscape: a software environment for integrated models of biomolecular interaction networks. *Genome Res*. 2003;13(11):2498–504.
17. Lucke-Wold BP, Logsdon AF, Manoranjan B, et al. Aneurysmal Subarachnoid Hemorrhage and Neuroinflammation: A Comprehensive Review. *Int J Mol Sci*. 2016;17(4):497.
18. Mo J, Enkhjargal B, Travis ZD, et al. AVE 0991 attenuates oxidative stress and neuronal apoptosis via Mas/PKA/CREB/UCP-2 pathway after subarachnoid hemorrhage in rats. *Redox Biol*. 2019;20:75–86.
19. Dykstra-Aiello C, Jickling GC, Ander BP, et al. Intracerebral Hemorrhage and Ischemic Stroke of Different Etiologies Have Distinct Alternatively Spliced mRNA Profiles in the Blood: a Pilot RNA-seq Study. *Transl Stroke Res*. 2015;6(4):284–9.
20. Stamova B, Ander BP, Jickling G, et al. The intracerebral hemorrhage blood transcriptome in humans differs from the ischemic stroke and vascular risk factor control blood transcriptomes. *J Cereb Blood Flow Metab*. 2019;39(9):1818–35.
21. Cheng X, Ander BP, Jickling GC, et al. MicroRNA and their target mRNAs change expression in whole blood of patients after intracerebral hemorrhage. *J Cereb Blood Flow Metab*. 2020;40(4):775–86.
22. Rosell A, Vilalta A, García-Berrococo T, et al. Brain perihematoma genomic profile following spontaneous human intracerebral hemorrhage. *PLoS ONE*. 2011;6(2): e16750.
23. Petzold GC, Windmüller O, Haack S, et al. Increased extracellular K⁺ concentration reduces the efficacy of N-methyl-D-aspartate receptor antagonists to block spreading depression-like depolarizations and spreading ischemia. *Stroke*. 2005;36(6):1270–7.
24. Zhu X, Tao L, Tejima-Mandeville E, et al. Plasmalemma permeability and necrotic cell death phenotypes after intracerebral hemorrhage in mice. *Stroke*. 2012;43(2):524–31.
25. Liang XM, Chen J, Zhang T, Liu J, Jiang XJ, Xu ZQ. Cerebral hemorrhage increases plasma concentrations of noradrenalin and creatine kinase MB fraction with induction of cardiomyocyte damage in rats. *Cell Biochem Biophys*. 2014;70(3):1807–11.
26. Zhou L, Deng L, Chang NB, Dou L, Yang CX. Cell apoptosis and proliferation in rat brains after intracerebral hemorrhage: role of Wnt/ β -catenin signaling pathway. *Turk J Med Sci*. 2014;44(6):920–7.
27. Liu L, Fuller M, Behymer TP, et al. Selective Serotonin Reuptake Inhibitors and Intracerebral Hemorrhage Risk and Outcome. *Stroke*. 2020;51(4):1135–41.
28. Walsh KB, Zhang X, Zhu X, et al. Intracerebral Hemorrhage Induces Inflammatory Gene Expression in Peripheral Blood: Global Transcriptional Profiling in Intracerebral Hemorrhage Patients. *DNA Cell Biol*. 2019;38(7):660–9.
29. Seiler K, Humbert M, Minder P, et al. Hexokinase 3 enhances myeloid cell survival via non-glycolytic functions. *Cell Death Dis*. 2022;13(5):448.
30. Stone JG, Rolston RK, Ueda M, et al. Evidence for the novel expression of human kallikrein-related peptidase 3, prostate-specific antigen, in the brain. *Int J Clin Exp Pathol*. 2009;2(3):267–74.
31. Poh AR, O'Donoghue RJ, Ernst M. Hematopoietic cell kinase (HCK) as a therapeutic target in immune and cancer cells. *Oncotarget*. 2015;6(18):15752–71.
32. Kong X, Liao Y, Zhou L, et al. Hematopoietic Cell Kinase (HCK) Is Essential for NLRP3 Inflammasome Activation and Lipopolysaccharide-Induced Inflammatory Response In Vivo. *Front Pharmacol*. 2020;11: 581011.
33. Wang Z, Ying C, Zhang A, et al. HCK promotes glioblastoma progression by TGF β signaling. *Biosci Rep*. 2020;40(6):BSR20200975.
34. Yamada M, Gomez JC, Chugh PE, et al. Interferon- γ production by neutrophils during bacterial pneumonia in mice. *Am J Respir Crit Care Med*. 2011;183(10):1391–401.
35. Zhang X, Cui Y, Ding X, et al. Analysis of mRNA-lncRNA and mRNA-lncRNA-pathway co-expression networks based on WGCNA in developing pediatric sepsis. *Bioengineered*. 2021;12(1):1457–70.
36. Tang S, Yu Q, Ding C. Investigational spleen tyrosine kinase (SYK) inhibitors for the treatment of autoimmune diseases. *Expert Opin Investig Drugs*. 2022;31(3):291–303.
37. Liu XY, Dai XH, Zou W, et al. Acupuncture through Baihui (DU20) to Qubin (GB7) mitigates neurological impairment after intracerebral hemorrhage. *Neural Regen Res*. 2018;13(8):1425–32.
38. Xie Y, Guo H, Wang L, et al. Human albumin attenuates excessive innate immunity via inhibition of microglial Mincle/Syk signaling in subarachnoid hemorrhage. *Brain Behav Immun*. 2017;60:346–60.
39. Sanderson MP, Lau CW, Schnapp A, et al. Syk: a novel target for treatment of inflammation in lung disease. *Inflamm Allergy Drug Targets*. 2009;8(2):87–95.
40. Alhazmi A. Spleen Tyrosine Kinase as a Target Therapy for *Pseudomonas aeruginosa* Infection. *J Innate Immun*. 2018;10(4):255–63.
41. Li Y, Liu S, Chen Y, et al. Syk Facilitates Influenza A Virus Replication by Restraining Innate Immunity at the Late Stage of Viral Infection. *J Virol*. 2022;96(7): e0020022.
42. Wu Z, Zhang Z, Lei Z, et al. CD14: Biology and role in the pathogenesis of disease. *Cytokine Growth Factor Rev*. 2019;48:24–31.
43. Xu H, Zhu Q, Tang L, et al. Prognostic and predictive value of FCER1G in glioma outcomes and response to immunotherapy. *Cancer Cell Int*. 2021;21(1):103.
44. Keller CW, Kotur MB, Mundt S, et al. CYBB/NOX2 in conventional DCs controls T cell encephalitogenicity during neuroinflammation. *Autophagy*. 2021;17(5):1244–58.
45. Mukherjee A, Epperly MW, Shields D, et al. Ionizing irradiation-induced Fgr in senescent cells mediates fibrosis. *Cell Death Discov*. 2021;7(1):349.
46. Girard R, Zeineddine HA, Koskimäki J, et al. Plasma Biomarkers of Inflammation and Angiogenesis Predict Cerebral Cavernous Malformation Symptomatic Hemorrhage or Lesional Growth. *Circ Res*. 2018;122(12):1716–21.
47. Elias-Oliveira J, Prado MKB, Souza COS, et al. CD14 signaling mediates lung immunopathology and mice mortality induced by *Achromobacter xylosoxidans*. *Inflamm Res*. 2022;71(12):1535–46.
48. Wang L, Lin Y, Yuan Y, et al. Identification of TYROBP and FCER1G as Key Genes with Prognostic Value in Clear Cell Renal Cell Carcinoma by Bioinformatics Analysis. *Biochem Genet*. 2021;59(5):1278–94.
49. Gu Y, Wu Y, Chen L. GP6 promotes the development of cerebral ischemic stroke induced by atherosclerosis via the FYN-PKA-pPTK2/FAK1 signaling pathway. *Adv Clin Exp Med*. 2021;30(8):823–9.
50. Wang X, Zeldin S, Shi H, et al. TAZ-induced Cybb contributes to liver tumor formation in non-alcoholic steatohepatitis. *J Hepatol*. 2022;76(4):910–20.
51. Gutkind JS, Robbins KC. Translocation of the FGR protein-tyrosine kinase as a consequence of neutrophil activation. *Proc Natl Acad Sci U S A*. 1989;86(22):8783–7.
52. Nelson MP, Metz AE, Li S, et al. The absence of Hck, Fgr, and Lyn tyrosine kinases augments lung innate immune responses to *Pneumocystis murina*. *Infect Immun*. 2009;77(5):1790–7.
53. Nelson MP, Christmann BS, Werner JL, et al. IL-33 and M2a alveolar macrophages promote lung defense against the atypical fungal pathogen *Pneumocystis murina*. *J Immunol*. 2011;186(4):2372–81.
54. Zhang G, Lu J, Zheng J, et al. Spi1 regulates the microglial/macrophage inflammatory response via the PI3K/AKT/mTOR signaling pathway after intracerebral hemorrhage. *Neural Regen Res*. 2024;19(1):161–70.

Publisher's Note

Springer Nature remains neutral with regard to jurisdictional claims in published maps and institutional affiliations.